Electromagnetic Torque Profile Improvement of An Interior Permanent Magnet Motor by VV Magnet Design

[1]Bui Minh Dinh, [2]Nguyen Viet Anh
[1]School of Electrical Engineering, Hanoi University of Science and Technologies
[2] Hanoi University of Industry-HUI

Abstract

This paper has compared double V-shape and Delta-shape rotor topologies by different optimal magnet angles. The power and torque are improved by changing the thickness of the outer bridge, and magnetic width. Various metamodels were generated for each of the multi-objective functions and constraints, and the metamodels with the best prediction performance were selected. By applying a multi-objective genetic algorithm, several optimal solutions were compared to those of the initial model. The proposed multi-objective optimization method can guide the design of IPMs for electric vehicles with high reliability and maximum torque. This program allows estimating electromagnetic torque, and ripple torque by analytical MATLAB program coupling to finite element magnetic method (FEMM) and GA optimization. Finally, rotor lamination was stamped and assembled in the motor for the back EMF test and no-load test. In order to evaluate the electromagnetic characteristic, a 2D FEM program has been implemented to compare with a commercial IPM motor from Roewe Marvel X AWD.

Keywords:
An Interior Permanent Magnet Motor.

1. Introduction

This paper will describe the design optimization of a three-phase IPM synchronous motor with double V-shape and Delta-shape rotor topologies. The aim of this paper is to investigate electromagnetic torque and power with the same active volume and weight of the commercial product of Roewe Marvel X AWD 85kW. The design optimization of the IPM motor is based on changing magnet geometry parameters in the rotor. Multi-objective optimization of maximum average torque and outpower is employed to design a 150 kW- IPM motor 48Slot/8poles with hairpin winding. Several parameters of stator diameter, slot depth, air gap, and magnet angle are variables. Mid-drive motors are known for higher performance and torque when compared to a similarly powered traditional hub motor. This design proposal will be applied to the middle drive motor for electrical cars. Technical parameters of this IPM have been summarized in table 1 and stator/rotor lamination in figure 1.

Table 1. IPM Specification

No	Parameters	Value
1	Peak power	150 kW
2	Hairpin Winding	15.729 kg
3	Rotor core	7.542 kg
4	Magnet	1.644 kg
5	Shaft	1.43 kg
6	End cap	1.44 kg
7	Total weight	31.613 kg
8	Voltage	350VDC

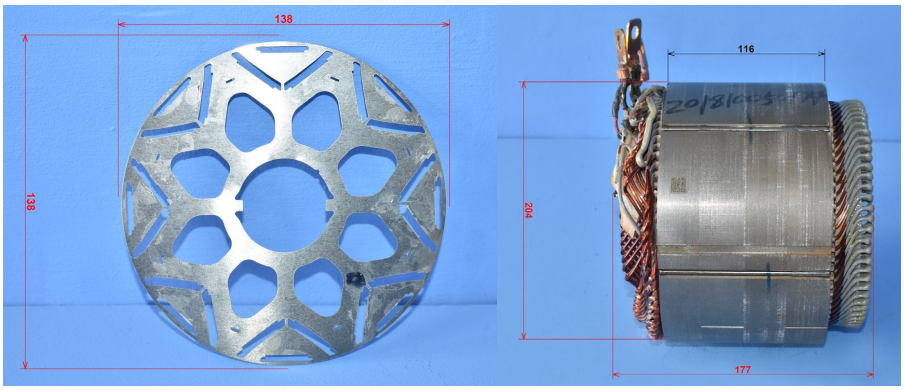

Figure 1. Stator and Rotor lamination of Roewe Marvel X AWD@85kW

2. Electromagnetic calculation

Electromagnetic torque has been calculated based on the stator, rotor diameter, and power inverter voltage and currents. The electromagnetic parameters can inertial calculated as:

$$T = \frac{\pi}{2} D^2 L_{stk} \sigma \,, \tag{1}$$

where T is the electromagnetic torque, D is the rotor diameter, L_{stk} is the stack length and $\sigma = \frac{L}{D}$ is defined from 0.8 to 1.25 for the inner rotor.

Torque prediction is carried out for any stator-rotor relative position and the finite element grid is automatically adjusted when the rotor is rotated. The influence of mesh has been investigated to get satisfactory accuracy avoiding inaccuracies due to element distortion. Only one pole is simulated, due to the motor symmetry.
The steady-state stator voltage equations written in the d-q rotating reference frame are:

$$\begin{aligned} v_d &= Ri_d - \omega L_q i_q \\ v_q &= Ri_q + \omega L_d i_d + \omega L_q i_q \end{aligned} \tag{2}$$

where: i_d , i_q , v_d and v_q are the d and q axis components of the armature current and terminal voltage respectively, R is the winding resistance per phase, L_d and L_q are the axis inductances and Φ is the magnets flux linked with the armature winding. The electromagnetic torque is calculated using the well-known equation.

$$T = \frac{3}{2} p \left[\phi_M i_q + \left(L_d - L_q \right) i_d i_q \right] \tag{3}$$

The study concerns V and Delta designs for a three-phase 85 kW, 8 poles, 48 slots, with a cross-section of the stator and rotor core shown in figure 2. The rotor presents one barrier per pole and the magnet material is inserted into this cavity. The stator and rotor consist of a stack of laminated high permeability non-oriented grain silicon steel. Three-phase double-layer hair windings are inserted in the 48 stator slots.

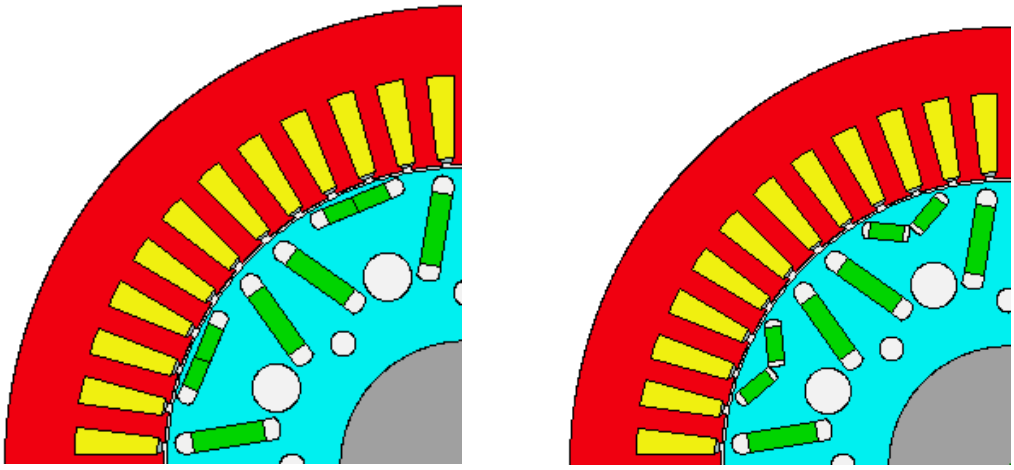

a. Delta Design b. VV Design

Figure 2. Delta and VV design

The Delta and VV designs need to satisfy several total material weight and dimensional constraints to guarantee reliability and feasibility in table 1. The main design constraint is the value of the back EMF at maximum speed which has not been allowed to exceed the rated terminal voltage 350VDC and maximum current density 20A/mm2. The main constraints are ratios of inner, outer stator/rotor, stator tooth and stator yoke, and stack length

Table 2. Delta and V weight

Components	**Materials**	**Density (kg/m3)**	**Delta design Weight (kg)**	**V design Weight (kg)**
Stator Lam (Back Iron)	M235-35A	7650	10.62	10.62
Stator Lam (Tooth)	M235-35A	7650	5.053	5.053
Stator Lamination [Total]			15.67	15.67
Armature Winding [Active]	Copper (Pure)	8933	2.225	2.225
Armature EWdg [Front]	Copper (Pure)	8933	0.8869	0.8869
Armature EWdg [Rear]	Copper (Pure)	8933	0.8869	0.8869
Armature Winding [Total]			3.998	3.998
Wire Ins. [Active]		1400	0.06908	0.06908
Wire Ins. [Front End-Wdg]		1400	0.02754	0.02754
Wire Ins. [Rear End-Wdg]		1400	0.02754	0.02754
Wire Ins. [Total]			0.1242	0.1242
Impreg. [Active]		1400	0.2043	0.2043
Impreg. [Front End-Wdg.]		1400	0.2448	0.2448
Impreg. [Rear End-Wdg.]		1400	0.3234	0.3234
Impreg. [Total]			0.7725	0.7725
Slot Wedge		1000	0.009423	0.009423
Slot Liner		700	0.0447	0.0447
Rotor Lam (Back Iron)	M350-50A	7650	3.022	3.022

Rotor Lam (IPM Magnet Pole)	M350-50A	7650	3.539	3.539
Rotor Lam (Inter Magnet Gap)		7650	0.3932	0.3932
Rotor Inter Lam (Back Iron)		1.127	1.32E-05	1.32E-05
Rotor Lamination [Total]			6.954	6.954
Magnet	N35UH	7500	1.647	1.647
Rotor Pocket		0.9461	8.77E-05	8.77E-05
Shaft [Active]	Stainless Steel 304	7900	2.591	2.591
Shaft [Front]	Stainless Steel 304	7900	0.3955	0.3955
Shaft [Rear]	Stainless Steel 304	7900	0.3568	0.3568
Shaft [Total]			3.343	3.343
Bearing [Front]		7800	0.1029	0.1029
Bearing [Rear]		7800	0.1029	0.1029
Flange Mounted Plate		2700	7.158	7.158
Total			**31.63**	**31.63**

The Finite Element analysis is used to evaluate the motor performance and the design requirements (at base speed and maximum speed), namely, to compute the objective function values and constraints of the minimization problem which represents mathematically the optimal design problem, and which considers the parameters of the motor as independent variables. The optimization procedure uses the information obtained by the FE program to iteratively update the set of motor parameters and try to identify an "optimal" motor by making a trade-off between the different parameters of the machine.

Table 3. Geometry parameters

1	48 Slots, 8 Poles
2	Shaft diameter = 60mm
3	Rotor outer diameter = 138 mm
4	Stator inner diameter = 139.4 mm
5	Airgap length = 0.7 mm
6	Stator stack length = 116 mm
7	Rotor stack length = 116.6 mm
8	Average stack = 116.3 mm

3. Optimization Algorithm

The set of parameters x used in the optimization procedure are listed in Table I. The motor has 8 variables (magnet length, outer stator diameter, air gap, slot depth and magnet angles) that vary in a discrete way. For good electromagnetic performance, it should be necessary to minimize irreversible demagnetization. The centrifugal force on steel bridges should be considered with maximum mechanical stress in high-speed operation. From a preliminary analysis, a minimum value of 2 mm is imposed. This value is consistent with the maximum speed and mechanical stress.

Table 4. Minimum and maximum variables

Parameters	**Discrete variables**	**min**	**max**	**step**
Magnetic Angle deg)	P1	100	150	3
Bridge Thickness layer 1 (mm)	P2	0.5	2	0.1
Bridge Thickness layer 2 (mm)	P3	0.5	2	0.1

Magnet gap (mm)	P4	0.5	1.5	0.1
Opening width (mm)	P5	2	5	1

An initial modeling and parametric analysis setting for the automatic change of design variables was performed using the FEA software SPEED. By creating Matlab files and batch files, electromagnetic analysis was automatically performed in SPEED. SPEED's analysis results were transferred to Matlab, and the responses of multi-objective functions and constraints were automatically calculated. In addition, when the computational analysis for one experimental point was finished, the shape design parameters were automatically changed in SPEED with the aid of CAD tools by receiving the MATLAB command. As described before, the optimal design of an IPM synchronous motor can be formulated as a particular multi-objective mixed-integer nonlinear programming problem. As regards the multi-objective aspect of the optimization problem, our numerical experience showed that, for this particular optimal design problem, a good compromise among different objectives can be obtained just by minimizing the sum of the weight of the motor and the opposites of the two torques. The general multi-objective optimization problem can be defined as find the finding or of parameters $x=[x_1, x_2,\ldots,x_n]$ and constraint functions $g_j(x)<0$ subject subjected D boundary constraints $x_{i\_min}<x<x_{i\_max}$, vector function $f(x)= [f_1(x), f_2(x),\ldots f_k(x)]$

$$\min f(x)$$
$$g(x) \le 0$$
$$\min \le x \le \max$$

The result of the optimization is a population of solutions that belong to a Pareto optimal set. In other words, the vectors of the Pareto set are not dominated by any other vector in the set. Since none of the vectors dominate, they are all equally good solutions that provide invaluable insight to the decision decision-maker to choose the best design to satisfy the performance criteria. The plot of the objective functions whose nondominant vectors are in the Pareto optimal set is called the Pareto front.

Table 5. Optimization Result

Parameter	Min	Max	Max Torque Variant	Reduced NVH Variant	Trade-off Variant
Lower Magnet Angle (P1)	45	53	49.674	51.328	50.521
Lower Magnet Barrier (P2)	4	5	4.573	4.214	4.327
Upper Magnet Barrier (P3)	0.8	1.2	0.8	0.906	0.951
Upper Magnet Separation (P4)	0.4	0.6	0.469	0.4	0.429
Slot Opening Thickness (P5)	1.8	2.4	2.384	2.322	2.191

The 150-kW prototype IPM motor has been designed using the multiobjective optimization algorithm previously described. The outer diameter of the stator core has been fixed in order to fit inside the standard aluminum cast frame of the motor manufacturer. The same has been done with the inner diameter of the rotor core to fit the standard shaft size.
Electromagnetic results of VV and Delta designs are compared in table 6. The efficiency and shaft torque of VV design is higher than the Delta design. The torque ripples are 2.6% in VV model and 9.54% in delta design because the VV magnet angle can be optimized.

Table 6. Electromagnetic result comparison

Parameters	**VV**	**Delta**	**Unit**
Maximum torque possible (DQ)	312.04	318.04	Nm
Average torque (virtual work)	303.16	309.34	Nm
Average torque (loop torque)	300.97	307.14	Nm
Torque Ripple (MsVw)	7.9349	29.347	Nm
Torque Ripple (MsVw) [%]	2.6201	9.5409	%
Cogging Torque Ripple (Ce)	1.0055	6.8577	Nm
Cogging Torque Ripple (Vw)	0.11478	2.747	Nm
Speed limit for zero q axis current	48198	53194	rpm
Electromagnetic Power	1.59E+05	1.61E+05	Watts
Input Power	1.64E+05	1.67E+05	Watts
Total Losses (on load)	6515.6	6606.8	Watts
Output Power	1.57E+05	1.60E+05	Watts
System Efficiency	96.968	96.033	%
Shaft Torque	308.71	305.47	Nm

Iron, copper, and addition losses of VV and Delta designs are compared in table 7. The total loss and of VV design is less than the Delta design with the same fiction, windage and stray losses

Table 7. Losses comparison

Parameters	**VV**	**Delta**	**Unit**
Armature DC Copper Loss (on load)	5483	5483	Watts
Magnet Loss (on load)	13.31	12.61	Watts
Stator iron Loss [total] (on load)	917.3	920.2	Watts
Rotor iron Loss [total] (on load)	201.6	190.7	Watts
Wedge Loss (on load)	43	43	Watts
Windage Loss (user input)	13	13	Watts
Friction Loss (user input)	11	11	Watts
Shaft Loss [total] (on load)	6.11E-07	2.11E-07	Watts
Total Losses (on load)	6606	6607	Watts

The variable electromagnetic torque vs angle at armature current is shown in Fig. 3. It can be seen that the higher the torque curve of VV design in comparison with Delta design. Fig 3 illustrates the electromagnetic torque profile. The torque is increase ranges from 150 N.m to 312 Nm at a root mean square (RMS) current 300A, respectively. The maximum torque is 312Nm with the angle of 50^0.

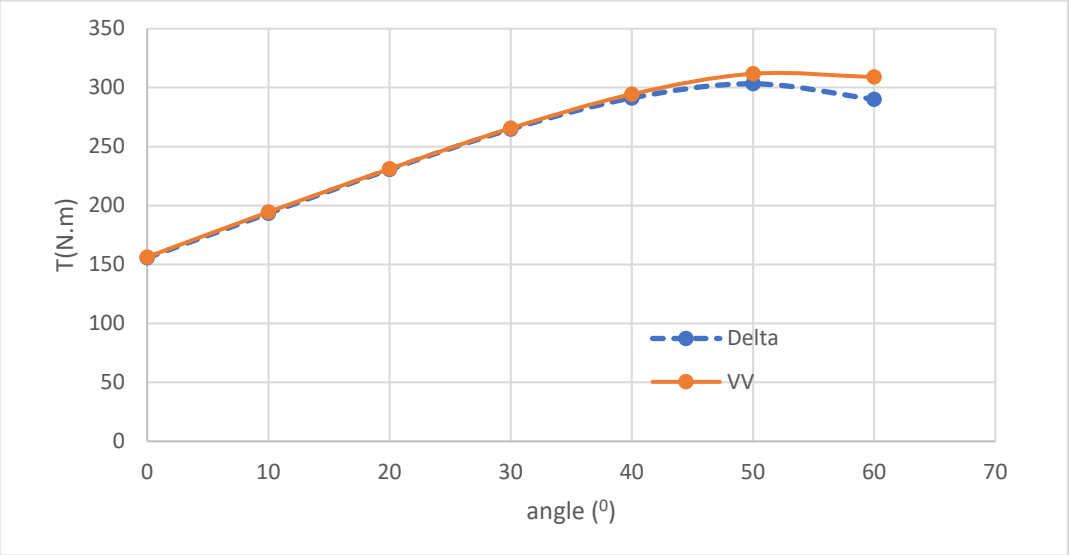

Figure 3. Torque vs angle curves

The purpose of rotor designing and building the prototype has been to investigate if the physical properties of the motor predicted in the design stage can be actually achieved in practice regardless of any design limitations dictated by the available magnet materials or the requirements for having specific motor dimensions. It is confirmed that the VV design is better and improved.

4. Thermal simulation

The losses during the duty cycle will be specified relative to the losses previously defined in the thermal model. This allows the losses to varying as given in the duty cycle and takes into account the variation in losses with speed and temperature. After solving the final transient circuit and temperatures can also be viewed in figure 5. The component colors in the schematic match those in the cross-section drawings. The maximum temperature is 107^0C lower than the limit temperature of 180^0C.

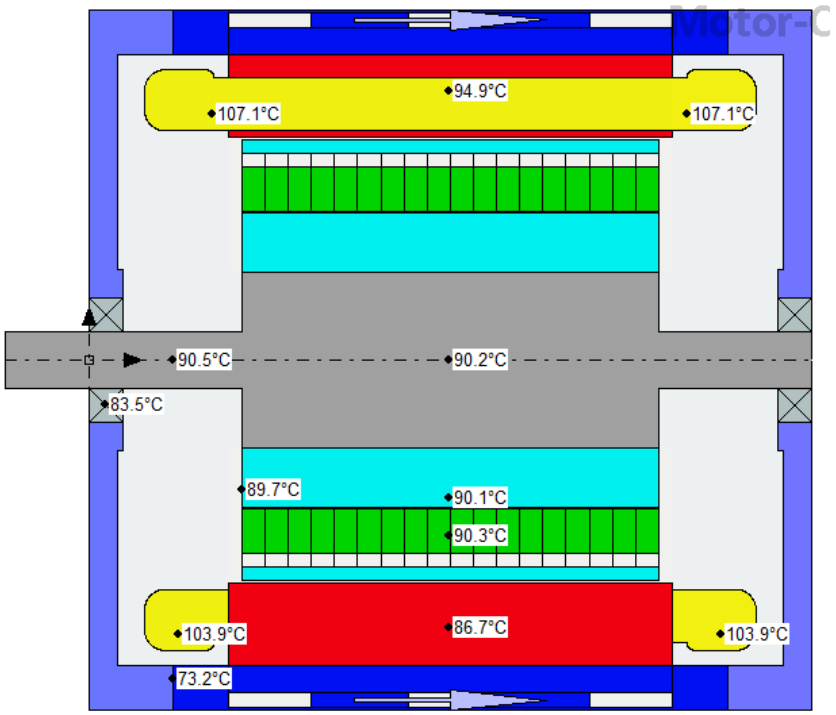

Figure 4. Temperature distribution in axial direction

Figure 5 shows the transient temperatures graph of the different components in the machine varies during the duty cycle.

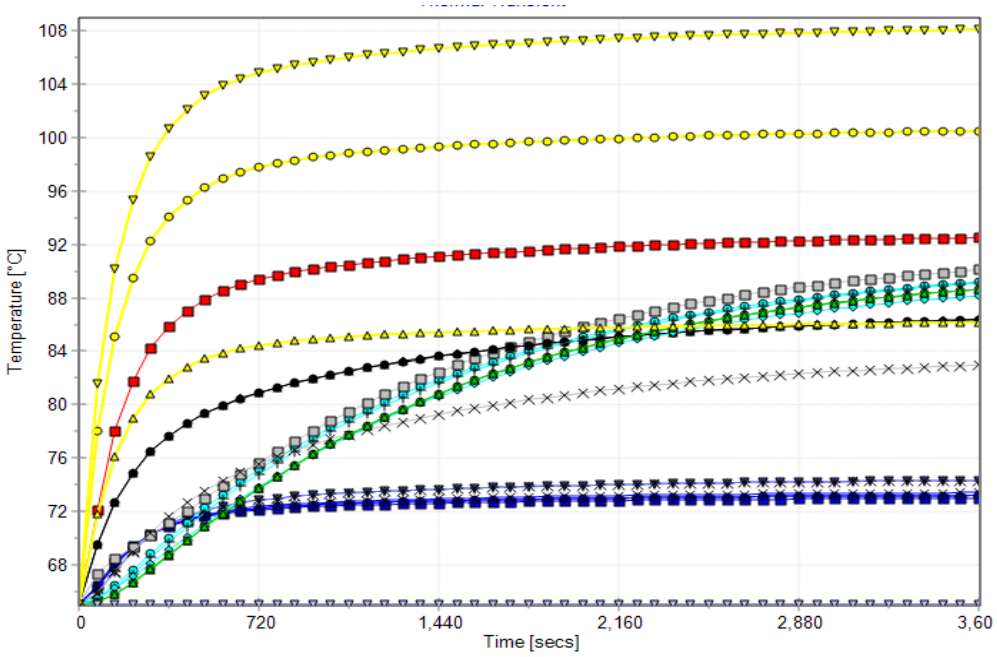

Figure 5. Transient temperatures graph

The transient temperatures graph shows how the temperatures of the different components in one hour**.** The plots are color coded to match the colors of the components shown in the plot, e.g. the yellow lines indicate the maximum winding temperatures

5. Conclusion

An effective analytical model is developed and verified with a prototype. To optimize the design process of the motor in a very short period and without any need of FEM an intelligent optimization algorithm is fully implemented and described. The result of optimization shows the efficiency of the entire approach. The analytical model and the optimization program are both implemented using MATLAB which makes it easier to use. To validate if the suggested motor truly meets the requirements and boundaries, results are verified using FEM which is also controlled via MATLAB and will be initiated automatically after optimization. The entire package is a very powerful tool for the optimized design of a permanent magnet synchronous motor. This paper has investigated and compared the performances of IPM with VV and delta in wide range speed for EV applications. A significant contribution of this study is an analytical calculation of VV magnet angle for improving electromagnetic torque. The simulation results can achieve the peak torque and 150 kW and 300 N.m at base speed of 5500 rpm for the VV model design.

ACKNOWLEDGMENT

This research was supported Selex Motor Company in Vietnam and Institute for Control Engineering and Automation- ICEA with Hardware test bench and Software.

REFERENCES

Hong, G.; Wei, T.; Ding, X. *"Multi-objective Optimal Design of Permanent Magnet Synchronous Motor for High Effciency and High Dynamic Performance"*. IEEE Access 2018

Edhah, S.O.; Alsawalhi, J.Y.; Al-Durra, A.A. "*Multi-Objective Optimization Design of Fractional Slot Concentrated Winding Permanent Magnet Synchronous Machines"*. IEEE Access 2019

Lee, J.H.; Kim, J.W.; Song, J.Y.; Kim, Y.J.; Jung, S.Y. "A Novel Memetic Algorithm Using Modified Particle Swarm Optimization and Mesh Adaptive Direct Search for PMSM Design", IEEE Trans. Magn. 2016

Shuangshuang Zhang;Wei Zhang;Rui Wang;Xu Zhang;Xiaotong Zhang, *"Optimization design of halbach permanent magnet motor based on multi-objective sensitivity",* CES Transactions on Electrical Machines and Systems, Year: 2020 | Volume: 4, Issue: 1 | Journal Article | Publisher: CES.

L. Zhai, T. M. Sun, and J. Wang, *"Electronic stability control based on motor driving and braking torque distribution for a four in-wheel motor drive electric vehicle,"* IEEE Trans. Veh. Technol., vol.65, no.6, pp. 4726-4739, Jun. 2016

X. Y. Zhu, Z. M. Shu, L. Quan, Z. X. Xuan, and X. Q. Pan, *"Design and multicondition comparison of two outer-rotor flux-switching permanent-magnet motors for in-wheel traction applications,"* IEEE Trans. Ind. Electron., vol.64, no.8, pp. 6137-6148, Aug. 2017

W. Fei, P. C. K. Luk, D.-M. Miao, and J. X. Shen, *"Investigation of torque characteristics in a novel permanent magnet flux switching machine with an outer-rotor configuration,"* IEEE Trans. Magn., vol.50, no.4, pp.1-10, Apr. 2014.

Y. Fan, L. Zhang, J. Huang, and X.D. Han, *"Design, analysis, and sensorless control of a self-decelerating permanent-magnet in-wheel motor,"* IEEE Trans. Ind. Electron., vol.61, no.10, pp. 5788-5797, Oct. 2014.

Y.F. Wang, H. Fujimoto, and S. Hara, *"Driving force distribution and control for electric vehicles with four in-wheel motors: a case study of*

acceleration on split-friction surfaces," IEEE Trans. Ind. Electron., vol.64, no.4, pp. 3380-3388, Apr. 2017.

Hwang, C.-C.; Cho, Y.H. "Effects of leakage flux on magnetic fields of interior permanent magnet synchronous motors". IEEE Trans. Magn. 2001, 37, 3021–3024

Ilka, R.; Alinejad-Beromi, Y.; Yaghobi, H. Techno-economic Design Optimisation of an Interior Permanent-Magnet Synchronous Motor by the Multi-Objective Approach. IET Electr. Power Appl. 2018, 12, 972–978.

Hong, G.; Wei, T.; Ding, X. Multi-objective Optimal Design of Permanent Magnet Synchronous Motor for High Effciency and High Dynamic Performance. IEEE Access 2018, 6, 23568–23581.

Cho, S.; Jung, K.; Choi, J. Design Optimization of Interior Permanent Magnet Synchronous Motor for Electric Compressors of Air-Conditioning Systems Mounted on EVs and HEVs. IEEE Trans. Magn. 2018, 54, 1–5

Lee, S.; Baek, S. A study on the improvement of the cam phase control performance of an electric continuous variable valve timing system using a cycloid reducer and BLDC motor. Microsyst. Technol. 2020, 26, 59–70

Ortega, A.J.P.; Paul, S.; Islam, R.; Xu, L. Analytical model for predicting effects of manufacturing variations on cogging torque in surface-mounted permanent magnet motors. IEEE Trans. Magn. 2016.

Zhou, Y.; Li, H.; Meng, G.; Zhou, S.; Cao, Q. Analytical calculation of magnetic field and cogging torque in surface-mounted permanent-magnet machines accounting for any eccentric rotor shape. IEEE Trans. Ind. Electron. 2015,